*Ceramics International* 23 (1997) 437–447

PII: S0272-8842(96)00052-1
0272-8842/97 $17.00 + 0.00

# Wear and Friction Behaviour of UHMWPE–Alumina Combination for Total Hip Replacement

**A. Chanda, A. K. Mukhopadhyay, D. Basu & S. Chatterjee**

Central Glass & Ceramic Research Institute, Jadavpur, Calcutta 700032, India

(Received 2 January 1995; accepted 27 March 1996)

**Abstract:** The wear and friction behaviour of ultra high molecular weight polyethylene (UHMWPE) against high purity fine grained alumina, the ideal material combination for total hip joint prosthesis, were studied under different contact pressures and sliding velocities using a pin-on-disc type wear and friction monitor. The wear heights in wet conditions were found to be much lower than those in dry conditions, which followed a power law relationship with load after 3·5 km of sliding. Efforts were also made to find out the sequence of dominating wear mechanisms. © 1997 Elsevier Science Limited and Techna S.r.l.

## 1 INTRODUCTION

Fully dense, high purity alumina is a well known bio-inert material, which is currently being used as the articulating component against ultra high molecular weight polyethylene (UHMWPE) in the artificial total hip replacement. High compressive strength, hardness and good bio-compatibility are the main advantages of alumina when used as a load-bearing component in bio-medical applications. The additional plus point for the alumina–polyethylene material combination is low wear and friction. However, during long term clinical trials, polymer debris of unwanted shape and size are accumulated at the artificial body joints. This results in macrophage activity, granulomatous tissue formation and necrosis of the bone surrounding the prosthesis,[1–4] leading to premature prosthetic loosening and subsequent failure.[5,6] Therefore, the need to develop better understanding of the tribological behaviour of alumina–polyethylene couple *in vivo*, as well as the pertinent wear mechanisms, assumes considerable technological importance, as well as societal implications.[7–9]

The wear rate of UHMWPE against alumina is reported to be much smaller compared to those against conventional articulating material of the hip joint, viz. stainless steel (SS316L) or Co Cr Mo alloy.[8–13] The reduced wear rate is thought to be linked to higher scratch resistance and superior wettability of alumina with liquids in comparison to those of the metallic implants. The lubricating effect of water and deposition of serum proteins to act as boundary lubricants on hard surfaces are two additional factors identified in connection to wear reduction.[14,15] Investigations on wear mechanisms of UHMWPE against stainless steel and alumina indicate the dominance of several processes either singularly or in combination with others.[16,17] These include abrasion and adhesion, micro-abrasion and surface fatigue, sub-surface slow crack growth, transfer film formation and back transfer phenomenon.[16–19]

The main objective of the present work was to investigate the tribological behaviour of UHMWPE against a commercial, bio-ceramic grade alumina in pin-on-disc configuration under dry and water lubricated conditions and to develop a qualitative understanding of the wear mechanisms involved. It is worth mentioning that this particular material has been used to prepare artificial total hip joints in our laboratory.

**Table 1. Chemical composition of disc material**

| Constituent | % |
|---|---|
| $Al_2O_3$ | 99.33 |
| $SiO_2$ | 0.09 |
| $Fe_2O_3$ | 0.06 |
| $TiO_2$ | Tr |
| CaO | Tr |
| MgO | Tr |
| $K_2O$ | Nil |
| $Na_2O$ | 0.05 |
| $ZrO_2$ | Nil |
| LOI | 0.35 |

Tr means trace.

**Table 2. Mechanical and physical properties of the disc material**

| | |
|---|---|
| Density (g./cc) | 3.94 |
| UTS (MPa) | 290 |
| Young's modulus (GPa) | 380 |
| Vicker's hardness (GPa) | 17.5 |
| Elongation at fracture (%) | — |

## 2 EXPERIMENTAL

### 2.1 Materials

The UHMWPE pins used in the present investigation were prepared from polyethylene (Hoechst RCH1000, surgical grade) produced by the Ziegler low pressure polymerisation method and it was supplied by Polypick India Ltd. The molecular weight was in the range of 2.5–3 million as per the manufacturer's data. The apparent density was measured to be 0.95–0.97 g/cc for the cylindrical pins of length 30 mm and diameter 6 mm. The opposite surfaces of the pins were ground parallel to each other and finally lapped to a surface finish (CLA) of 0.5 $\mu$m. The quality of the finish was monitored by a profilometer (Surtronic 3P, Form Talysurf Plus, Rank Taylor Hobson Ltd, UK). The ceramic disc was prepared from calcined alumina with the characteristics given in Table 1. The disc surface was polished to a CLA value of 0.6 $\mu$m. Grain size measurement was carried out by the line-intercept method applied to a scanning electron micrograph of a polished, etched section. The average grain size was $4.02 \pm 0.08$ $\mu$m with a range of 3–5 $\mu$m, which is in complete agreement with the recommendation (ASTMF83 603) for biomedical orthopaedic usage of alumina ceramic. The physical and mechanical properties of the disc are listed in Table 2.

**Table 3. Test conditions in unidirectional wear and friction monitor**

| Test conditions | Pin-on-disc wear |
|---|---|
| Contact surface area ($mm^2$) | 28.26 |
| Contact stress (MPa) | 0.35, 0.70, 1.05, 1.42 |
| Sliding speed (m/min) | 62.5, 95.0, 125.0 |
| Room temperature (°C) | 25 |

### 2.2 Methods

The ceramic disc was fitted to the rotating disc in the plexiglass chamber in a pin-on-disc type unidirectional wear and friction monitor (Fig. 1). The

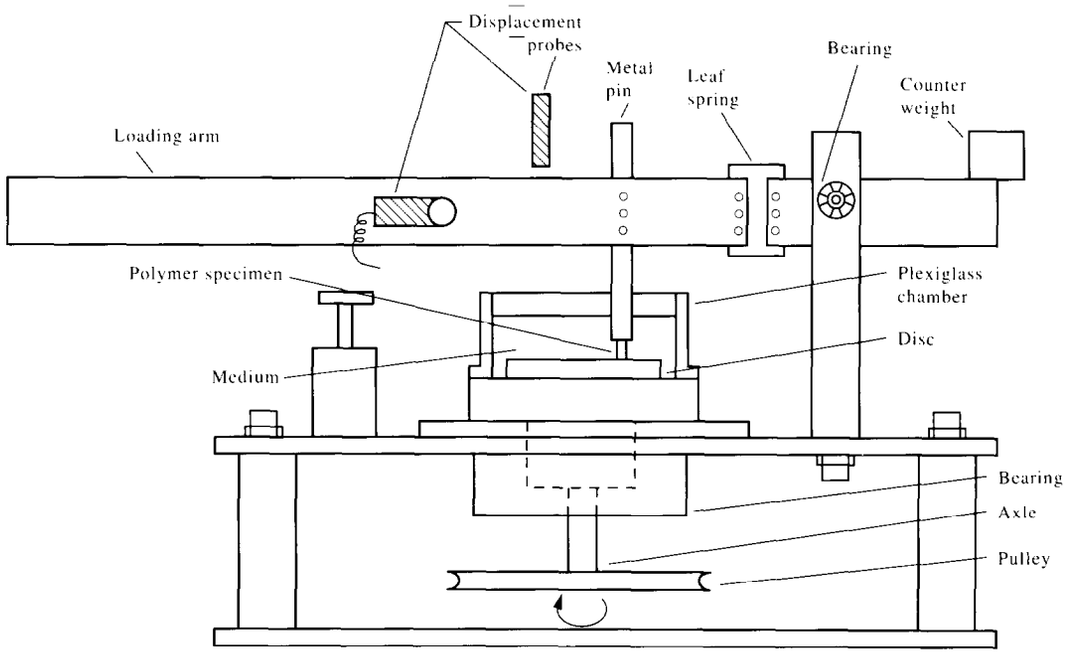


**Fig. 1.** Outline diagram of unidirectional wear and friction testing machine.

polyethylene pin was fitted to the holder. Load was provided by hanging weights at the end of the lever arm, connected to the holder. A variable speed electric motor was used to rotate the counterface disc in a counter-clockwise direction. The different test conditions are listed in Table 3.

Wear of the polyethylene pin was estimated by the decrease in the pin height, recorded by an LVDT with an accuracy of $\pm 1\,\mu$m. Wear factors were also calculated from the reduction in pin height and gravimetric estimations using the following expression:

$$W = V/(P \times S) \tag{1}$$

where $W$ is the wear factor, $V$ is the volumetric wear, $P$ is the load on the pin and $S$ is the distance slid. The frictional force was measured by a load cell and the coefficient of friction was calculated from the following equation:

$$f = F/P \tag{2}$$

where $f$ is the coefficient of friction, $F$ is the tangential force and $P$ is the load on the pin. As it was often reported that polyethylene undergoes a fair amount of creep deformation under load,[10,16] the pins were subjected to constant axial loads for hours before the commencement of wear tests. This helped to eliminate errors in the instantaneous measurement of wear height.

## 3 RESULTS

### 3.1 Creep of UHMWPE

Figures 2(a) and (b) show the creep data of the polyethylene pins in air and in water. The polymer deformed appreciably during the initial 1–2 h and thereafter creep became almost constant. The absolute values of creep under different loads were found to be higher in water than in air. For both type of tests, transition to an insignificant deformation region occurred at around 3 h for average loads, while for high loads small variation still occurred up to about 4–5 h. In water lubricated conditions, creep values were found by subtracting the increase in linear dimension due to absorption of water [Fig. 2(c)]. From the figures it is clear that to estimate wear the polymer specimens have to be kept under loads for >5–6 h before actual wear tests. To be on the safe side, the polymer pins were subjected to axial loads for 10–12 h to remove creep.

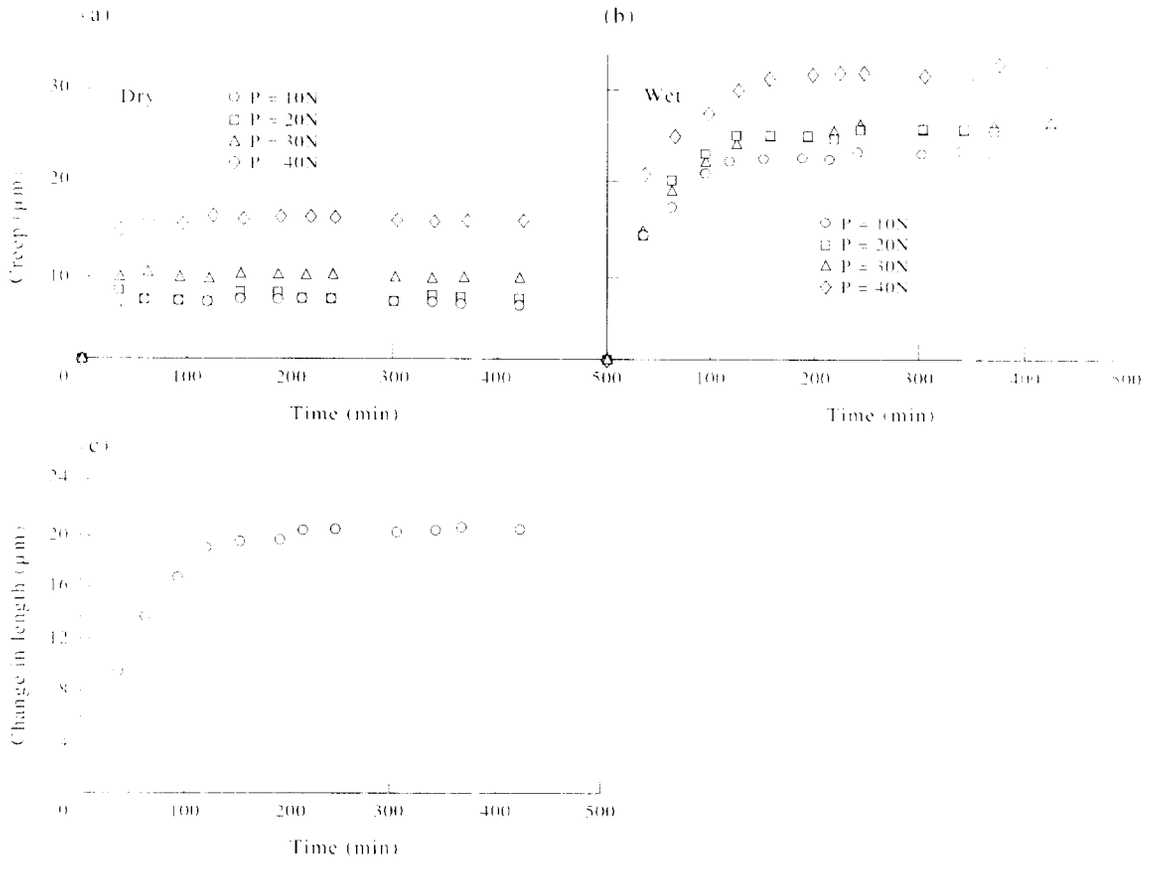


**Fig. 2.** Creep of UHMWPE in (a) dry and (b) wet conditions. (c) Variation in length of UHMWPE pin with time due to absorption of water.

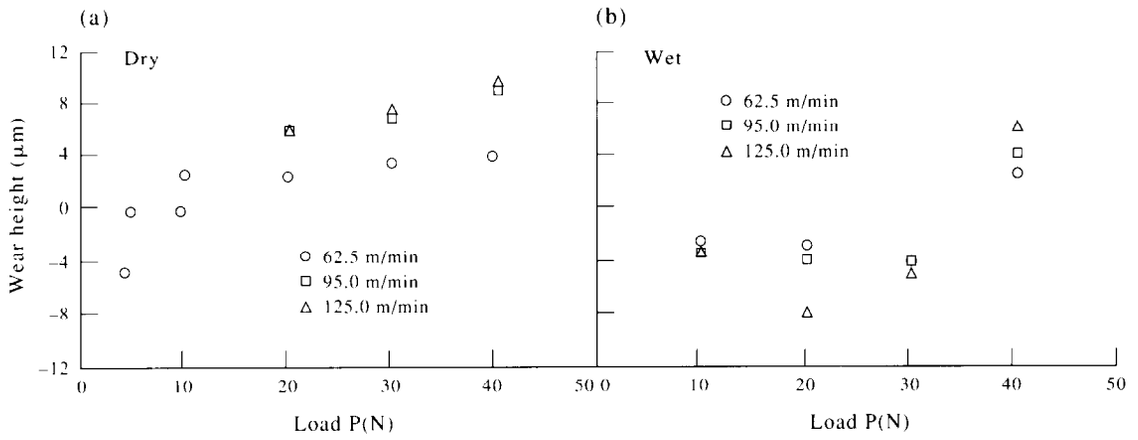


**Fig. 3.** Variation of wear height with load in (a) dry and (b) wet conditions.

### *3.2 Wear characteristics*

#### *3.2.1 Effect of normal load*

The data on variation of wear height as a function of normal loads for different sliding speeds are shown in Fig. 3(a) and (b) for dry and wet tests. The total time of sliding was 2 h for each case. In dry sliding the general trend was an empirical power law dependence of wear height on load. The power law variation was prominent from around a sliding distance of 3–5 km. In the wet tests, however, the trend was exponential in nature with respect to load.

#### *3.2.2 Effect of sliding distance*

Figures 4(a)–(d) and 4(e)–(h) show the data on variation of wear height as a function of sliding distance under four different normal loads and at three different sliding speeds for dry and wet tests, respectively. At low loads ($P < 20$ N), the wear height did not change significantly in dry tests after a sliding distance of 4 km at the lowest sliding speed. For higher speeds, the knee of this trend shifted to slightly higher sliding distances, e.g. 6–8 km [Fig. 4(a)–(d)]. For a given sliding distance and load, higher speed caused higher wear. This trend was more prominent in the case of high loads, e.g. 40 N [Fig. 4(d)]. In wet tests, a peak in wear height was followed by a gradual reduction at higher sliding distances. The extent of reduction was to vary with the load on the pin [Fig. 4(e)–(h)]. The peak position shifted to higher sliding distances for higher speeds for all normal loads. For a combination of low load and low speed [Fig. 4(f)] the amount of wear was almost insignificant.

#### *3.2.3 Wear factors*

The wear factor remained nearly constant for loads $< 20$ N prior to marginal reduction at still higher loads in the dry tests [Fig. 5(a)]. In wet tests, the wear factor initially declined with load [Fig. 5(b)] prior to a sharp rise after a load of 30 N. The overall average wear factors were $5.5 \times 10^{-7}$ mm$^3$/N.m for dry tests and $3.1 \times 10^{-7}$ mm$^3$/N.m for wet tests.

### *3.3 Friction characteristics*

Figures 6(a)–(d) and 6(e)–(h) show the data on the friction coefficient as a function of sliding distances for different speeds and loads for both dry and wet tests, respectively. In general, the values gradually reduced with distance. The trend of dependence of friction coefficient on either load or sliding speed was much less prominent for the wet cases than in dry ones. The range of variation of friction coefficient as a function of sliding distance, along with parametric variation of load and speed, was also much narrower for wet cases.

### *3.4 Deformation features*

Pre- and post-wear features for the same portion of the polymer pin surface in dry tests are shown in Fig. 7(a) and (b), respectively. Here the load was 40 N, the distance slid was 10 km and the speed was 125 m/min. A series of abrasive scratch marks were observed along the direction of sliding [Fig. 7(b)]. An SEM study of the same polymer cross-section clearly indicated the closely spaced scratch marks, along with a polymer particle [Fig. 8(a)]. The enlarged view of the particle [Fig. 8(b)] showed even smaller particles on it, indicating the continuity of the accumulation process. The polymer transfer and its adherence to the disc (as shown in Fig. 9) was observed in all loads and speeds, in dry as well as water lubricated conditions.

### *3.5 Surface topography*

Figures 10(a) and (b) show the typical surface profiles prior to wear test for the alumina disc and

polymer pin surface, respectively. Post-wear profilometry reveals that the disc became smoothened with time: from an initial CLA value of 0.93 $\mu$m for a particular small zone on the wear track, it went down to 0.72 $\mu$m for the same zone. For the polymer pin, it decreased from an initial value of 0.5 $\mu$m (CLA) to a final value of 0.41 $\mu$m (CLA). But as the amplitude of the asperity heights on both the surfaces and their distribution strongly affect the magnitude of interfacial loads, their orientations and, consequently, the tribological behaviour of the couple, Kurtosis values were also calculated along with CLA values of the surfaces. The Kurtosis values of the disc surface (listed in Table 4) indicate that a smooth and flat profile was the result of wear.

The transferred polymer layer was also studied by a profilometer and a typical profile is shown in Fig. 11. The profile indicated that towards the centre of the wear track accumulation increased, though some sporadic presence of a deep valley was also noticed midway along the path. The maximum height of the transferred layer was in the range 15–18 $\mu$m.

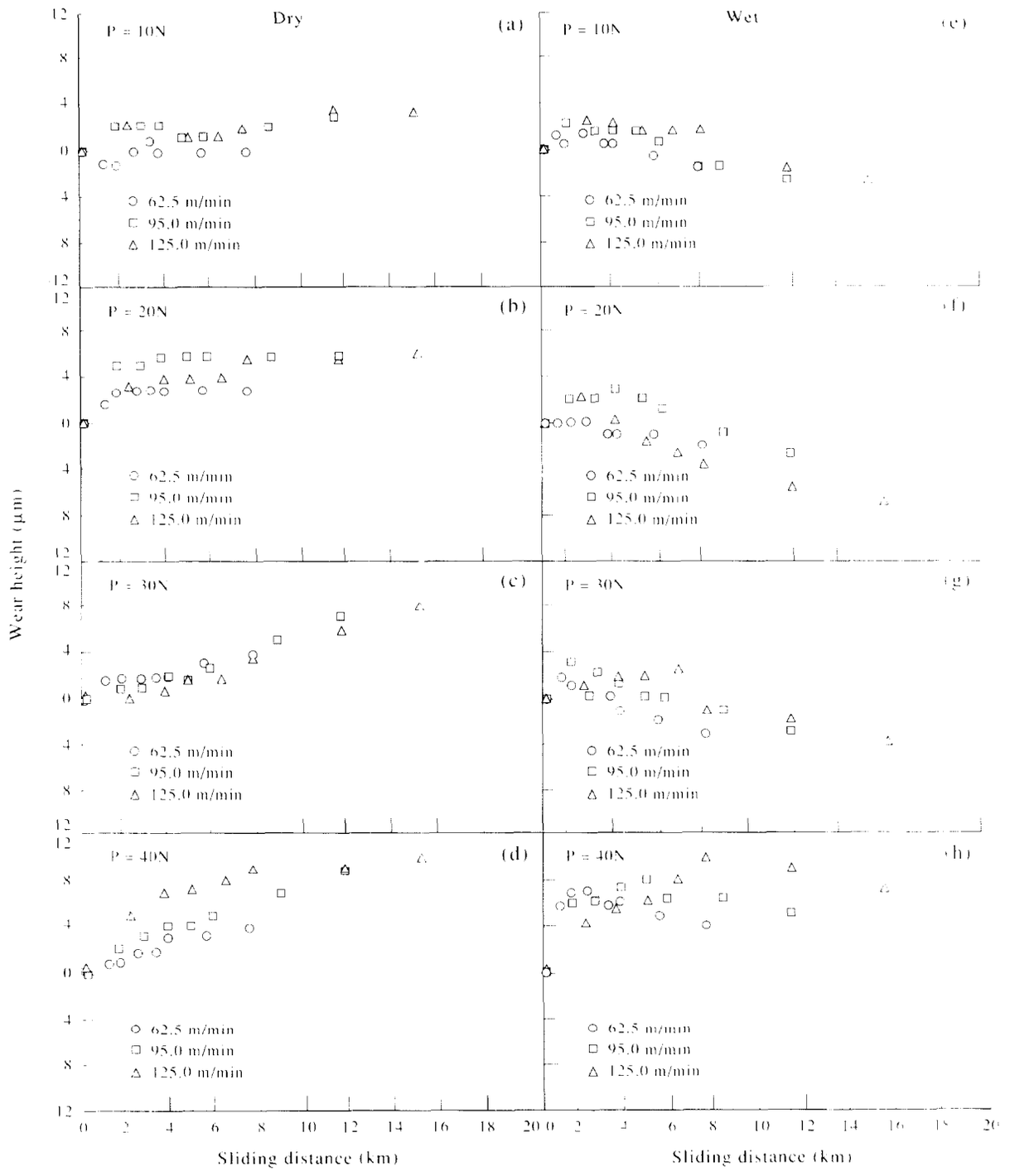


**Fig. 4.** Variation of wear height with sliding distance in dry [(a)–(d)] and wet [(e)–(h)] conditions.

## 4 DISCUSSION

### 4.1 Wear and friction characteristics

There are two major aspects of the present results which need to be discussed. One is the variation of wear height with normal load, speed and sliding distance, while the other is the wear mechanisms.

In the dry tests, it has been mentioned that wear height increased with increase in load in a power law fashion. High load increased abrasive action, as well as the intimacy between the surfaces. Naturally, the probability of junction formation resulting in adhesive wear also increased with increasing sliding distance. Increase in load raised temperature at the interface, which might have an effect on the properties and counterface. Consequently, a number of events, like oxidation of surfaces, third body wear by entrapped particles, etc., might occur. Due to the presence of such

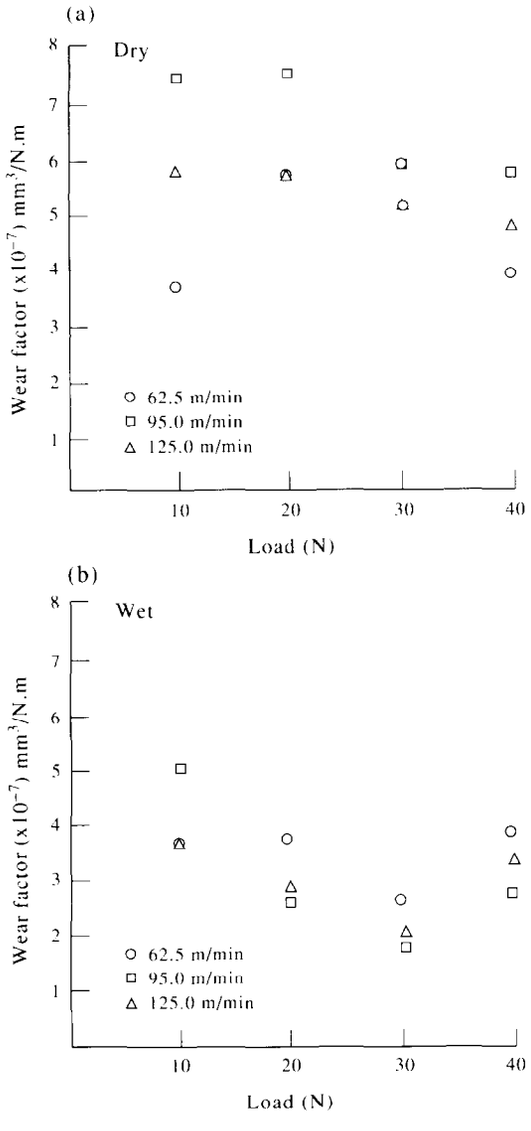


**Fig. 5.** Variation of wear factor with load in (a) dry and (b) wet conditions.

complicating load-dependent phenomena, the particular law (power) of variation of wear height with load as observed here should be considered to be applicable to this particular geometric arrangement of sliding and over this definite range of load and speed. In water lubricated cases, the wettability of alumina with liquid created an interfacial fluid film which separated the surfaces effectively to reduce wear and no definite law of variation occurred. With higher sliding speed, wear height increased in almost all the cases in dry sliding. An increase in interfacial temperature due to frictional heating with increase in speed might have caused this. In the liquid environment, a cooling action obviously occurred and such dependence was not observed. The nature of variation of wear height with sliding distance, the various deformation features and surface topographical study confirms that no single wear mechanism acted throughout the whole sliding path.

During the initial phase of dry sliding, the surface of the polymer pin was likely to undergo a fair amount of plastic deformation. This happened as softer polymer asperities were pressed against the hard, smooth ceramic counterface. A similar type of macroscopic polymer asperity deformation mode was also reported by others.[20] From the theory of Greenwood and Williamson[21] for the occurrence of this type of deformation, the plasticity index, $w$, was calculated by the following equation:

$$w = (\sigma/r)^{0.5}(E/H) \tag{3}$$

where $\sigma$ is the standard deviation of the distribution of asperity heights from the mean line, $r$ is the radius of the asperity peak, $H$ is the hardness of the softer material, and $E$ is the equivalent elastic modulus of the concerned material combination, given by:

$$E = [(1 - \nu_1^2)/E_1 + (1 - \nu_2^2)/E_2]^{-1} \tag{4}$$

Here $\nu_1$ and $\nu_2$ stand for the Poisson's ratios of the materials, and $E_1$ and $E_2$ for their respective modulus of elasticity.

**Table 4. Surface parameters of the ceramic disc**

| | Centre line average (CLA) ($\mu$m) | Kurtosis ($\mu$m) |
|---|---|---|
| Dry: | | |
| Initial reading | 0.6 | 7.230 |
| Final reading | 0.13 | 1.769 |
| Wet: | | |
| Initial reading | 0.6 | 8.420 |
| Final reading | 0.09 | 1.120 |

The value of $w$ as calculated from different material properties (Table 1) was found to be 2.45, which denotes that plastic deformation was very likely to occur.

In addition to this, abrasive ploughing action by the hard ceramic asperities were also very likely to occur as the surface topography clearly indicates that the asperity height varied from 2 to 10 $\mu$m on the counterface. From the theory of Hutchings[22] for polymer–ceramic combinations, the hard counterface must posses a CLA value greater than a few microns to cause abrasive scratching on the softer counterpart. In the present case, though the CLA value was small, the heights of the asperities were sufficient to plough through the polymer. The small area of contact at the tip of the ceramic asperity at different loads created pressure, of the order of 10–50 GPa, as the tip radius was found to be in the range of 12–25 $\mu$m from surface profilometry. Initial deformation of polymer asperities enhanced this ploughing action by providing intimate contact between the surfaces.

But this does not prevail throughout the whole sliding path. The intimacy of contact between the ceramic and polymer surfaces led to a possibly parallel process of adhesive bonding. The origin of this bonding might be the electrostatic interaction, including the van der Waal's type forces between

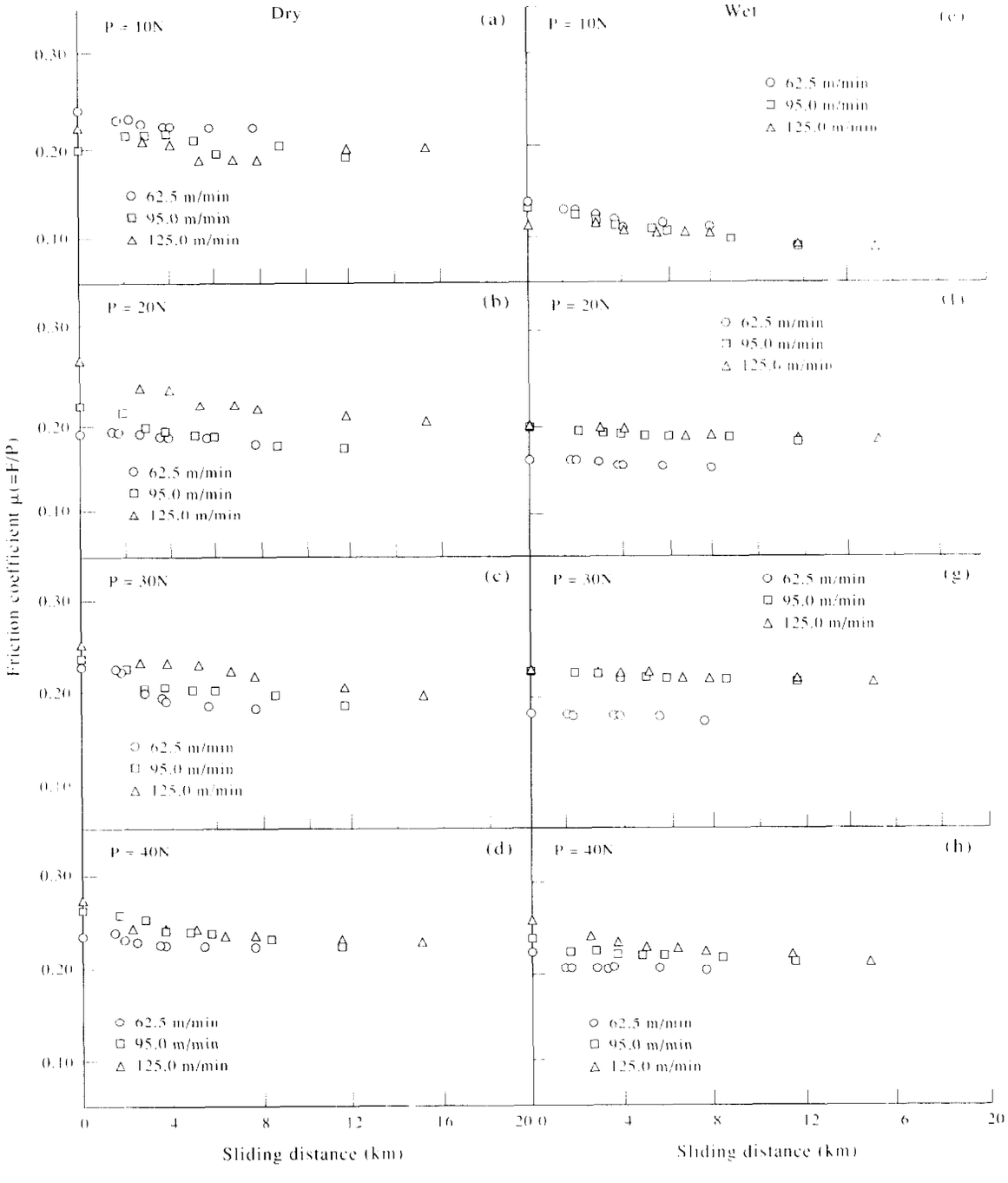


**Fig. 6.** Variation of coefficient of friction with sliding distance in dry [(a)–(d)] and wet [(e)–(h)] conditions.

the surfaces in close proximity.[22] These adhesive bonds promoted the formation of adhesive junctions. Due to the relative motion, a high shearing component of stress developed at the interfacial region. As the strength at the bond was likely to be higher than that in the bulk polymer, shear assisted process of crack initiation and its subsequent propagation under sustained loading led to the detachment of thin polymer fragments from the polymer pin. These fragments adhered to the ceramic disc to form a transfer layer as observed experimentally (Fig. 9). A similar type of transfer phenomenon has also been reported by others.[19] Due to repetitive sliding contact under pressure, an underlying process of fatigue might have acted as well.

The development of the transfer layer had both quantitative and qualitative implications on the tribological performance and wear mechanisms. With time the transfer layer progressively developed and coated the ceramic disc. Thus, the initial ceramic–polymer contact was gradually replaced by a polymer–polymer contact which reduced the effective counterface hardness and the contribution of abrasive component to overall wear. Moreover, the uniformity in the distribution of polymer filled up the depressions between the asperities and increased the area of contact, which reduced local stress and consequently wear. Hence, with an increase in sliding distance the wear rate reduced and gradually became almost constant.

Based on the present experimental results and the aforesaid discussions, we would like to propose the following sequence of the occurrence of wear mechanisms, as shown in Fig. 12.

Firstly, the deformation of polymer asperities occurred due to the pressure exerted by the hard

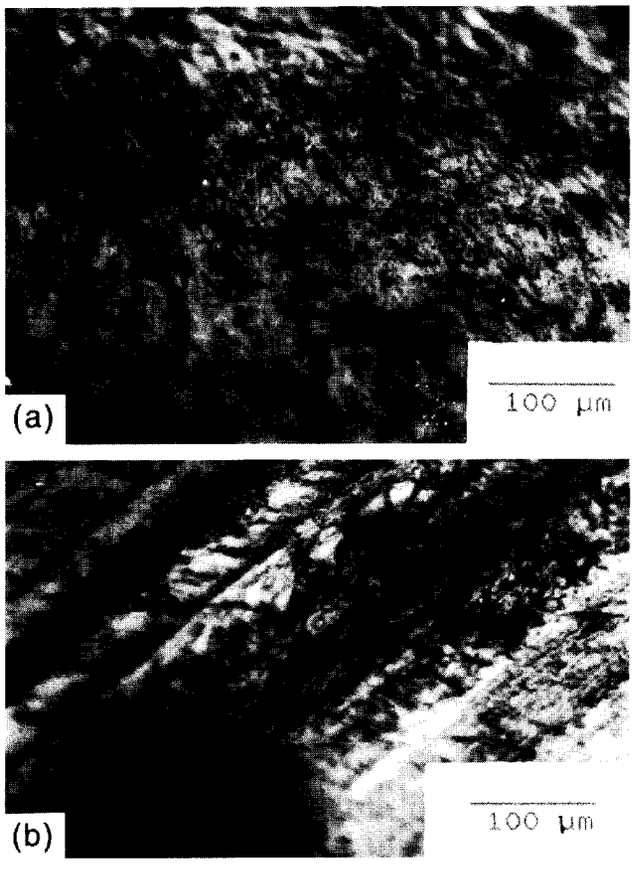


**Fig. 7.** Optical microscopic view of polymer pin surface before (a) and after (b) dry sliding wear.

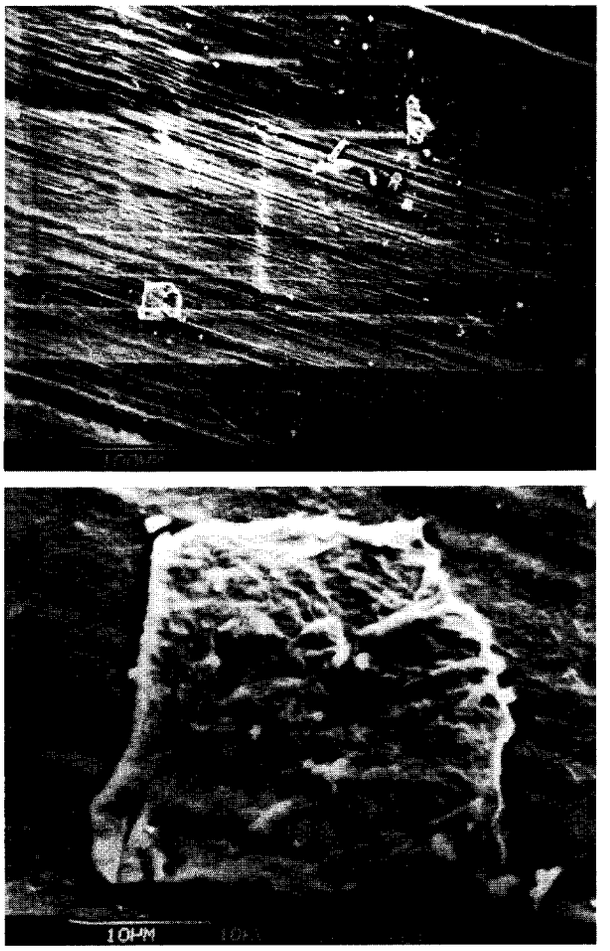


**Fig. 8.** Scanning electron microscopic view of (a) worn out polymer pin surface and (b) loose polymer fragment.

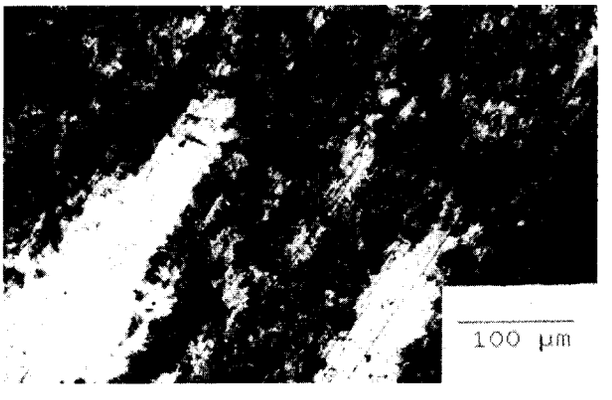


**Fig. 9.** Optical microscopic view of transferred polymer layer.

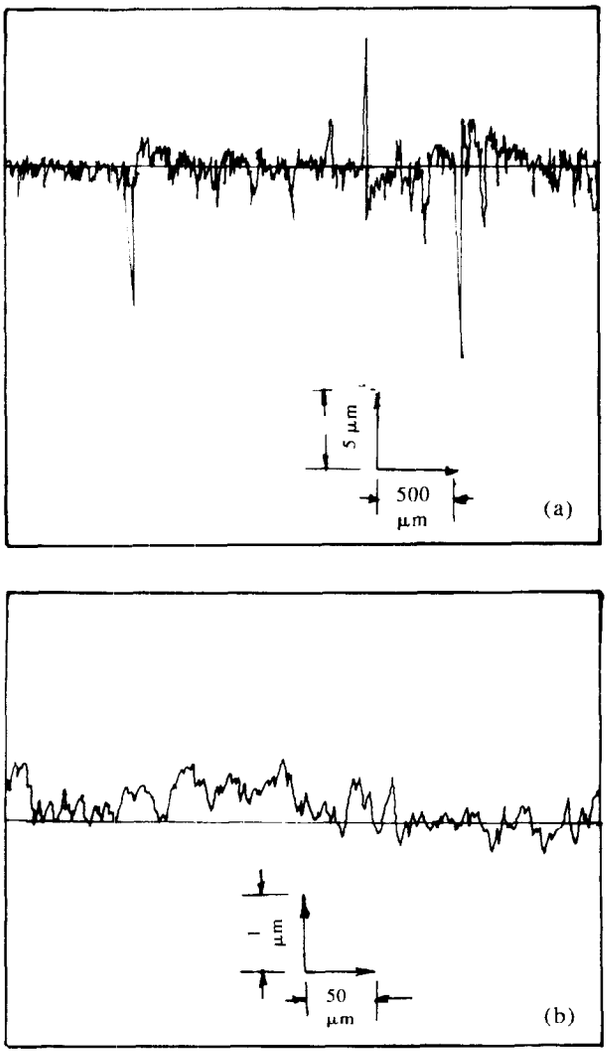


Fig. 10. View of profiles of (a) alumina disc and (b) polymer pin before wear.

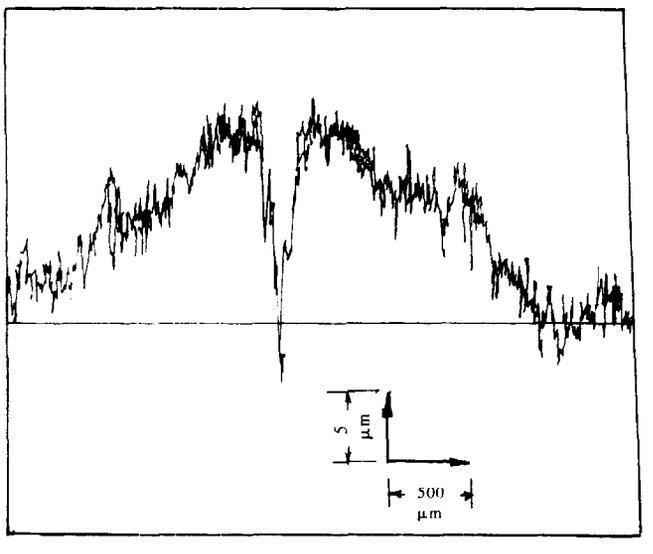


Fig. 11. View of surface profile of the transferred polymer layer across the wear track.

ceramic disc [Fig. 12(a)–(c)]. This was supplemented by the ploughing action by the ceramic asperities of heights greater than a few microns. With time, the deformed and flattened polymer came into better contact with the ceramic disc and, consequently, more and more hard protuberances ploughed through the polymer [Fig. 12(d)–(f)]. Some polymer particles might stick to the ceramic asperities to reduce the effectivity of abrasion as well. The abrasive action lasted for a definite time span depending on the load on the pin and the sliding speed. Afterwards, as the ceramic surface came into even closer confirmity with the polymer, an adhesive form of junction making and breaking occurred [Fig. 12(g)–(i)]. This type of wear dominated for the remaining portion of the experiment, with its severity gradually decreasing with progressive development of the transfer film. Though some definite mechanisms are being proposed, it is to be noted that no clear-cut demarkation line between the zones of their occurrence should be drawn, rather the region of dominance of a particular mechanism supplemented by others can be shown (Fig. 13).

In the water lubricated condition, the exact wear mechanism seemed to be complex in nature and not yet fully understood. The very low wear height of the polymer might be due to the good wettability of alumina with a polar liquid like water. The occurrence of negative wear values was due to greater uniformity in the transfer of polymer which displaced the pin upwardly, showing negative wear heights recorded by the LVDT. The transfer of polymer indicates that some sort of adhesive bonding might have occurred, even in the water flooded situation. Besides, with higher loads, the uniformity of the transfer film was pronounced. Probably with time and high loads the lubricating film got impaired locally and the asperities came into close contact with the polymer surface to pick up fragments or to cause junction formation.

It was felt, though, that further detailed study would be needed before these conjectures regarding wear mechanism can be amply confirmed.

## 5 CONCLUSION

With a view to understand the tribological behaviour and wear mechanisms, unidirectional pin-on-disc type wear tests were conducted with a bio-ceramic grade alumina disc and UHMWPE pins in both dry and water lubricated conditions. The results enable us to draw the following major conclusions:

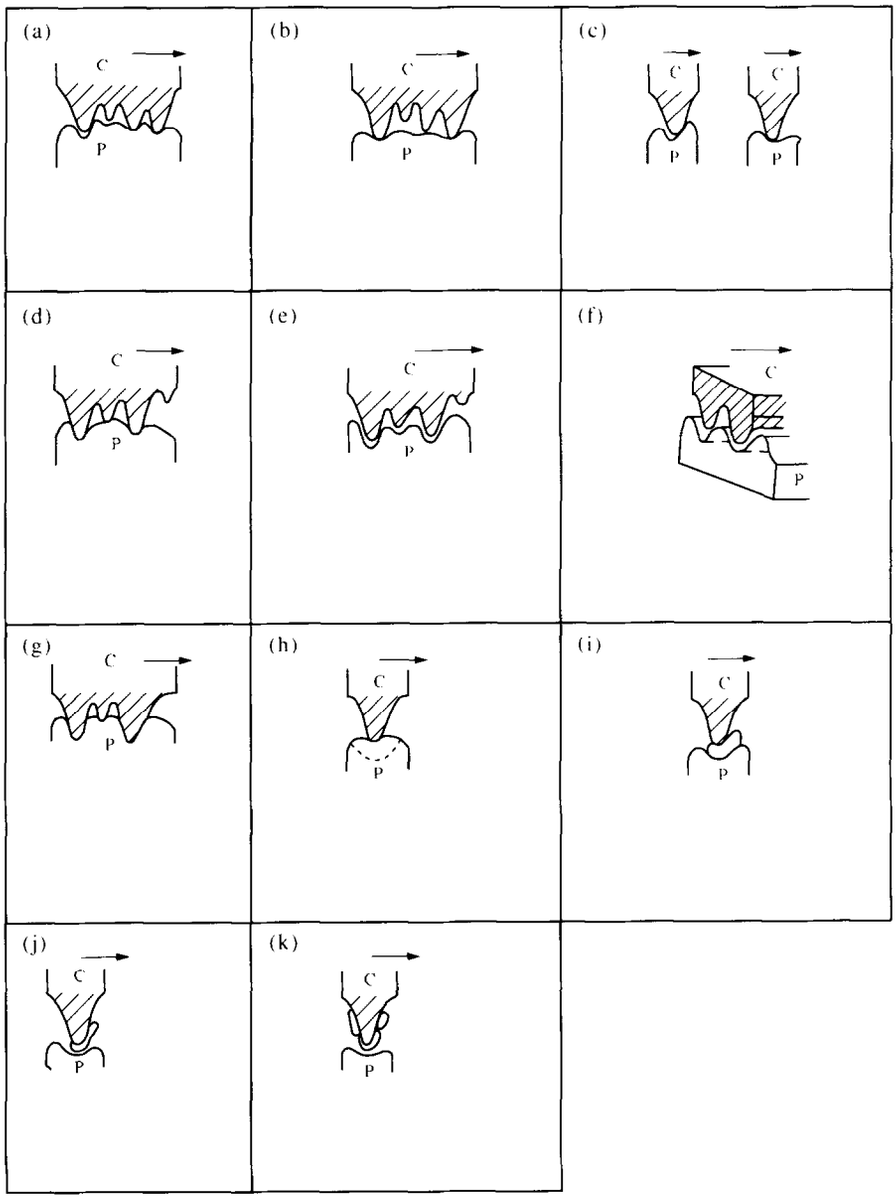


**Fig. 12.** Schematic representation of different wear events: (a) primary ceramic (C)–polymer (P) contact; (b),(c) deformation of polymer asperity; (d) enhanced contact between polymer and ceramic. (e),(f) ploughing action by ceramic asperities; (g)–(i) adhesive transfer: "junction making and breaking"; (j),(k) formation of polymer coating on ceramic asperity.

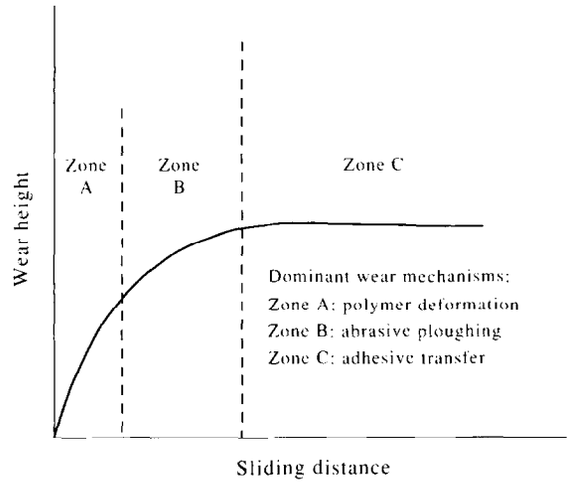


**Fig. 13.** Changes in wear mechanisms of UHMWPE–alumina combination with sliding distance.

1. Corresponding to present experimental conditions, creep of the polymer pin becomes negligible after 6 h in both dry and wet tests.
2. In dry tests, wear heights showed a power law dependence on load after a sliding distance of 3–5 km. Wear height also increased with sliding speed.
3. Wear heights in water lubricated conditions were very low in comparison to those in dry cases due to the good wettability of alumina with polar liquids.
4. Plastic deformation of polymer asperities and ploughing action by the ceramic asperities dominated the initial phase of sliding path. However, at longer sliding distances, an adhesive component of wear with transfer film

phenomenon occurred. The gradual development of a transfer film and its distribution over the ceramic disc reduced wear and friction with time.

5. The average overall wear factor in water lubricated condition was smaller by a factor of 2 than that in dry cases. A similar type of reduction in coefficient of friction occurred with water lubrication.

## ACKNOWLEDGEMENTS

The authors are grateful to the Director, CGCRI for his kind permission to publish this paper. One of the authors (A. Chanda) thanks D.S.T., Government of India for financial assistance. Thanks are also due to D.K. Naskar, L.K. Naskar, S. Mazumdar and S. Mandal for technical help.

## REFERENCES

1. WILLERT, H. G. & SEMLITSCH, M., Reactions of the articular capsule to wear products for artificial joint prostheses. *J. Biomed. Mater. Res.*, **11** (1977) 157–164.
2. REVELL, P. A., WEIGHTMAN, B., FREEMAN, M. A. R. & ROBERTS, B. V., The production and biology of polyethylene wear debris. *Arch. Orthop. Trauma Surg.*, **91** (1978) 167–181.
3. CLARKE, I. C. & CAMPBELL, C., Interface failure dynamics. In *Progress in Bioengineering*, ed. J. P. Paul. Adam Hilger Publ., Bristol, UK, 1989, pp. 104–115.
4. HOWIE, D. W., ROBERTS, B. V., OAKESHOTT, R. & MANTHEY, B., The rat model of bone resorption at the cement–bone interface in the presence of polyethylene wear particles. *J. Bone Joint Surg.*, **70A** (1988) 256–263.
5. LENNOX, D. W., SCHOFIELD, B. H., MCDONALD, D. F. & RILEY, L. H., A histological comparison of aseptic loosening of cemented press fit and biologic ingrowth prosthesis. *Clin. Orthop. Rel. Res.*, **225** (1987) 171–191.
6. MIRRA, J. H., MARDER, R. A. & AMSTUTZ, H. C., The pathology of failed total joint replacement. *Clin. Orthop. Rel. Res.*, **170** (1982) 175–183.
7. DOWSON, D. & LINNET, I. W., A study of wear of UHMWPE against alumina ceramic. In *Mechanical Properties of Biomaterials*, ed. G. W. Hastings & D. F. Williams. John Wiley, New York, 1980, pp. 3–25.
8. MCKELLOP, H., CLARKE, I., MARKOLF, K. & AMSTUTZ, H., Friction and wear properties of polymer, metal and ceramic prosthetic materials evaluated on a multichannel screening device. *J. Biomed. Mater. Res.*, **15** (1981) 619–633.
9. WEIGHTMAN, B. O., PAUL, I. G., ROSE, R. M., SIMON, S. R. & RADIN, E. L., A comparative study of total hip replacement prosthesis. *J. Biomech.*, **6** (1983) 299–311.
10. FISHER, J. & DOWSON, D., Tribology of total artificial joints. *Proc. Inst. Mech. Engrs.* **205** (1991) 73–79.
11. FISHER, J. & LIGHT, D., The effect of surface finish of alumina and stainless steel on the wear rate of UHMW polyethylene. *Biomaterials*, **7** (1986) 20–29.
12. OKUMURA, H., YAMAMURO, T., KUMAR, P., NAKAMURO, T. & OKA, M., Socket wear in total hip prosthesis with alumina ceramic head. In *Bioceramics, Proc. 1st Int. Bioceramic Symp. Vol. 1*, ed. H. Oonishi, H. Aoki & K. Sawai. Ishiyaku Euro America, Tokyo, 1984, pp. 284–289.
13. KAWACHI, K., KUROKI, Y., SAITO, S., OHGIYA, H., SATO, S., KONDO, S., HIROSE, I., OBARA, S., YAMANO, K., SASADA, S. & NOROSE, S., Total hip endoprosthesis with ceramic head and HDPE socket, clinical wear rate in orthopaedic ceramic implants. In *Proc. Jpn Soc. Orthop. Ceramic Implants, Vol. 4*, ed. H. Oonishi & Y. Ooi. Ishiyaku Euro America, Tokyo, 1984, pp. 253–257.
14. SEMLITSCH, M., LEHMANN, M. & WEBER, H., New prospects for a prolonged functional life span of artificial hip joints by using material combination polyethylene/aluminium oxide ceramic/metal. *J. Biomed. Mater. Res.*, **11** (1977) 537–552.
15. KUMAR, P., OKA, M., IKEUCHI, K., SHIMIZU, K., YAMAMURO, T., OKUMURO, H. & KOTOURA, Y., Low wear rate of UHMWPE against zirconia ceramic (Y PSZ) in comparison to alumina ceramic and SUS316L. *J. Biomed. Mater. Res.*, **25** (1991) 813–828.
16. MCKELLOP, H., CLARKE, I. C., MARKOLF, K. I. & AMSTUTZ, H. C., Wear characteristics of UHMWPE: A method for accurately measuring extremely low wear rates. *J. Biomed. Mater. Res.*, **12** (1978) 895–927.
17. ATKINSON, J. R., DOWSON, D., WROBLEWSKI, B. M. & ISAAC, G. H., Laboratory wear tests and clinical observations of femoral heads in acetabular cups. *Wear*, **104** (1985) 205–244.
18. SIEBER, H. P. & WEBER, B. G., HDPE/Ceramic Total Hip Replacement: The St Gallen *in vivo* and *in vitro* Experience. In *Ceramics in Surgery*, ed. P. Vincenzini. Elsevier, Amsterdam, 1983.
19. COOPER, J. R., DOWSON, D. & FISHER, J., Birefringent studies of polyethylene wear specimens and acetabular cups. *Wear*, **151** (1991) 391–401.
20. COOPER, J. R., DOWSON, D., FISHER, J., ISAAC, G. H. & WROBLEWSKI, B. M., Observations of residual subsurface shear strain in the ultra high molecular weight polyethylene acetabular cups of hip prosthesis. *J. Mater. Sci., Mater. in Med.*, **5** (1994) 52–57.
21. GREENWOOD, J. A. & WILLIAMSON, J. B. P., Contact of nominally flat surfaces. *Proc. Roy. Soc. Lond.*, **A295** (1966) 300–319.
22. HUTCHINGS, I. M., *Tribology: Friction and Wear of Engineering Materials*. Edward-Arnold, London, 1989.